LNF-92/076

Unoccupied electron states of Ni, Mo, and $MoNi_3$ alloy

M.T. Czyżyk, K. Ławniczak-Jablońska, S. Mobilio

Physical Review B45, n.4, 1581-1589 (1992)

Unoccupied electron states of Ni, Mo, and $MoNi_3$ alloy

M.T. Czyżyk
Research Institute of Materials, University of Nijmegen, Toernooiveld, NL-6525 ED Nijmegen, The Netherlands

K. Ławniczak-Jabłońska
Institute of Physics, Polish Academy of Sciences, aleja Lotników 32/46, PL-02668 Warsaw, Poland

S. Mobilio
Laboratori Nazionali di Frascati dell' Instituto Nazionale de Fisica Nucleare, via Enrico Fermi 40, I-00044 Frascati, Italy and Università de L'Aquila, Roio Monteluco-L'Aquila, Italy

(Received 6 May 1991)

We report on a systematic study of the unoccupied electronic states of long-range-ordered orthorhombic $MoNi_3$ alloy as well as its parent metals as reference. Measurements included the bremsstrahlung isochromat spectra for incoming-electron kinetic energy of 5414 eV and K-edge x-ray-absorption spectra of Ni. Further, all measured spectra were calculated on the basis of *ab initio* band-structure calculations performed for the investigated materials. The influence of the core hole on the Ni K-edge absorption spectrum was found to be small. A substantial deviation of the local structure in the long-range-ordered alloy was inferred by analogy to a local deformation of the lattice in semiconducting pseudobinary (ternary) alloys.

I. INTRODUCTION

Much attention in the literature has been devoted to the studies of the occupied electron states in solids. Fast development of commercially available x-ray and ultraviolet photoelectron spectrometers offers attractive experimental facilities for their investigation and comparison with theoretical results.

Nowadays, x-ray synchrotron radiation facilities also make possible good quality, highly resolved measurements of x-ray absorption spectra (XAS). The development in photoelectron spectroscopy stimulates the bremsstrahlung isochromat measurements.[1,2] Easy access to these two techniques, which probe the unoccupied density of states (DOS), has created an increase of interest in calculations that can provide the unoccupied DOS distribution in a wide range of energy. Calculations of x-ray absorption and isochromat spectra from first principles using a band-structure approach require knowledge of the conduction-band energies and wave function up to relatively high energies. This results in considerable complexity of the calculations because of the large number of energy levels in the high-energy regions of the spectra. From the experimental point of view, no single technique compares directly the calculated DOS with measured data. In fact, each technique involves additional effects which change the observed DOS distribution. Therefore, a comparison of several methods employed to measure the same material offers the possibility to examine the importance of these additional effects.

X-ray absorption spectroscopy is a symmetry- and site-projecting technique. Proper choice of edges can provide the partial DOS projected on each site. On the other hand, the many-body response to the creation of a core hole (correlation effects) can change significantly[3,4] the single-particle picture. On the other hand, the bremsstrahlung-isochromat-spectra (BIS) method is free from core-hole effects. For this reason comparison of the BIS and XAS allows us to estimate the importance of the core-hole potential. However, BIS is not site projecting and mixes contributions from different partial states which makes the comparison somewhat involved. For many years it was assumed that there is no important dependence of isochromat spectra on the transition matrix elements involved in the process.[5] There is, however, ample evidence now (see, e.g., Refs. 6 and 7) that this assumption is not valid. Nevertheless, the lack of a realistic calculation of the transition matrix elements is a serious limitation in attempts to perform an accurate analysis of the intensity distribution in the isochromat spectra, since only a few such calculations in the wide energy range can be found in the literature.[6–9]

In this work we present x-ray absorption measurements at the K edge of Ni in $MoNi_3$ ordered alloy and wide energy range measurements of isochromat spectra of this alloy. The same measurements were also done for elemental Ni and Mo to obtain a proper reference in our study. Furthermore, we report *ab initio* electronic-band-structure calculations for both metals and for the alloy. In order to calculate the unoccupied DOS in the energy range higher than a few electron volts above the Fermi level, it was found necessary to go beyond the minimal basis set[10] employed by the standard linearized methods of band calculations, i.e., linear muffin-tin orbital (LMTO) and augmented spherical waves (ASW). For this reason the localized-spherical-wave (LSW) method[11] with the extended basis set[12,13] was used in this work. This method allowed us to extend first-principles calcula-

tions up to 70 eV above Fermi level. The calculated and measured spectra give an excellent overall match for the pure metals. The importance of additional effects in XAS and BIS for these materials is assessed. In the case of the intermetallic $MoNi_3$ compound the situation is much more complex. From a comparison of our theoretical and experimental data we suggest that the local structure in ordered $MoNi_3$ alloy is different from its long-range structure in the way they differ in the pseudobinary (ternary) II-IV and III-V semiconducting alloys.

The paper is organized to report the experimental details in Sec. II. Then the essential information about the electronic structure calculations performed in this work is given in Sec. III. Next, Sec. IV contains a step-by-step comparison of theoretical and experimental results together with emerging conclusions. Finally, in Sec. V we summarize our work.

II. EXPERIMENT

The samples of Ni and Mo were thin metal foils of high-purity Goodfellow Metals. Polycrystalline $MoNi_3$ samples were prepared from metal foils by repeated arc melting of weighted amounts of the materials in a helium atmosphere. The x-ray microprobe was used to check the chemical composition at several different surface regions. The samples were cut into 0.5–1.0-mm-thick slices. To form the orthorhombic long-range ordered structure the samples were annealed four days at a temperature of 1013 K. The structure was controlled by x-ray diffraction. The long-range-order coefficient was estimated to be equal to 0.84. The samples were powdered in order to facilitate x-ray diffraction and absorption measurements.

XAS at the K edge of Ni were collected using the x-ray beam line of the PULS facility at Frascati Synchrotron Radiation Laboratory. The radiation coming out from the Adone storage ring working at 1.5 GeV and $I = 50$ mA was monochromatized by a Si(111) channel-cut crystal. The geometrical resolution was 1.5 eV. Two ion chambers were used for the detection of the x-ray beam before and after the sample. The spectra for Ni were recorded at steps of 0.6 eV in the absorption and fluorescence modes. The spectrum for $MoNi_3$ alloy was recorded only in fluorescence mode.

BIS were measured at a photon energy of 5415 eV. A Si(220) Johann-type monochromator was set at the Cr $K\alpha$ line (5414.72 eV). A proportional counter was used as an x-ray detector. The energy of the electron beam was changed in the case of Mo by 0.2-eV steps and in the case of Ni and alloy by 0.5-eV steps. The energy resolution of the isochromat spectrometer estimated from the BIS spectra of Pd was equal to 1.8 eV.[9] The electron beam current was 10 mA. The vacuum in the x-ray tube was of the order of 10^{-4} Pa.

The samples were mechanically polished using emery paper and ultrasonically washed in acetone then mounted on a water-cooled holder and kept during measurement at about 1000 K, to avoid carbon and oxygen contamination and in the case of the alloy sample, changes in atomic order. We did not notice any influence of surface contamination on the measured BIS. The isochromat spectrum registered for Ni was very similar to the spectrum registered by Chu and Best[6] in a vacuum better than 10^{-8} Pa.

III. ELECTRONIC STRUCTURE CALCULATION

Powder x-ray diffraction of the ordered $MoNi_3$ alloy proves that the alloy crystallized in the orthorhombic close-packed structure which belongs to the space group $Pmmn(D_{2h}^{13})$.[14,15] The unit cell, with parameters a =5.064, b =4.224, and c =4.488 Å, contains eight atoms in the following Wyckoff position:

$$\text{Mo}\ \ 2a\ (0,0,z_a)\ \ \text{with}\ z_a = \tfrac{1}{2} + z_c,$$
$$\text{Ni}\ \ 2b\ (0,\tfrac{1}{2},z_b)\ \text{with}\ z_b = 1 - z_a,$$
$$\text{Ni}\ \ 2f\ (x,0,z_c)\ \ \text{with}\ z_c = 0.0157\ \text{and}\ x = \tfrac{1}{4}.$$

These data were the relevant input parameters in *ab initio* band-structure calculations, carried out by the LSW method.[11] We used the scalar-relativistic Hamiltonian (spin-orbit interaction not included) with exchange and correlation effects treated within the local (spin) density approximation using (spin-polarized) Hedin-Lundqvist parametrization. The self-consistent calculations were performed including all core electrons and with the minimal basis set of augmented spherical waves (SW) for the valence electrons containing 5*s*-, 5*p*-, and 4*d*-like functions for Mo, and 4*s*-, 4*p*-, and 3*d*-like functions for Ni.

The most commonly used linearized methods of band-structure calculation LMTO, ASW-LSW, and linear augment plane wave were designed for an optimal description of occupied valence states. By optimal we mean here both accuracy and efficiency in self-consistent calculations. However, all these methods show a deficiency of the basis set when attempting to describe unoccupied electron states in the energy range higher than the first few eV above Fermi energy or above the bottom of the conduction band in the case of insulators.[12] In order to avoid the disadvantages of inelegant energy paneling techniques used in the linearized methods to overcome this deficiency, we used the extended basis set option[12] of the LSW method.[11] Operationally, it works as follows. The self-consistency is achieved with the minimal basis set as defined above. Then, the set is enlarged and unoccupied eigenstates of the self-consistent potential are recalculated in a much wider energy range. In our case, we added the following augmented SW to the basis set: for Mo, 4*f*-, 5*d*-, and 6*s*-like functions; and for Ni, 4*f*-, 4*d*-, and 5*s*-like functions.

The self-consistent iteration was carried out with 64 **k** points uniformly distributed in an irreducible part of the Brillouin zone (IBZ) which is equivalent to 343 points in the whole BZ. Then the Hamiltonian was diagonalized with the extended basis set and the linear tetrahedral integration technique was used to obtain the partial DOS.

To have a reference in our analysis, the calculations of the band structure of elemental Mo and Ni were performed by the same method with the same level of ac-

curacy (that implies that equivalently more **k** points in the IBZ were used) and using the same basis sets as for atoms Mo and Ni in the alloy. Such calculations, as a matter of fact, are trivial nowadays and the results are well known (see, e.g., Ref. 16), so no further details will be given here.

In Fig. 1 we show the local partial DOS of the ordered orthorhombic $MoNi_3$ alloy. Discussion of the structure of occupied valence states together with relevant experimental results (x-ray photoemission spectroscopy and x-ray emission spectroscopy) will be given elsewhere.[17] One may, however, already notice here the modification of these states when compared with the partial states of the parent metals Mo and Ni given in Fig. 2 also in the wide energy range. In this paper we concentrate on unoccupied states and in the next section the x-ray absorption

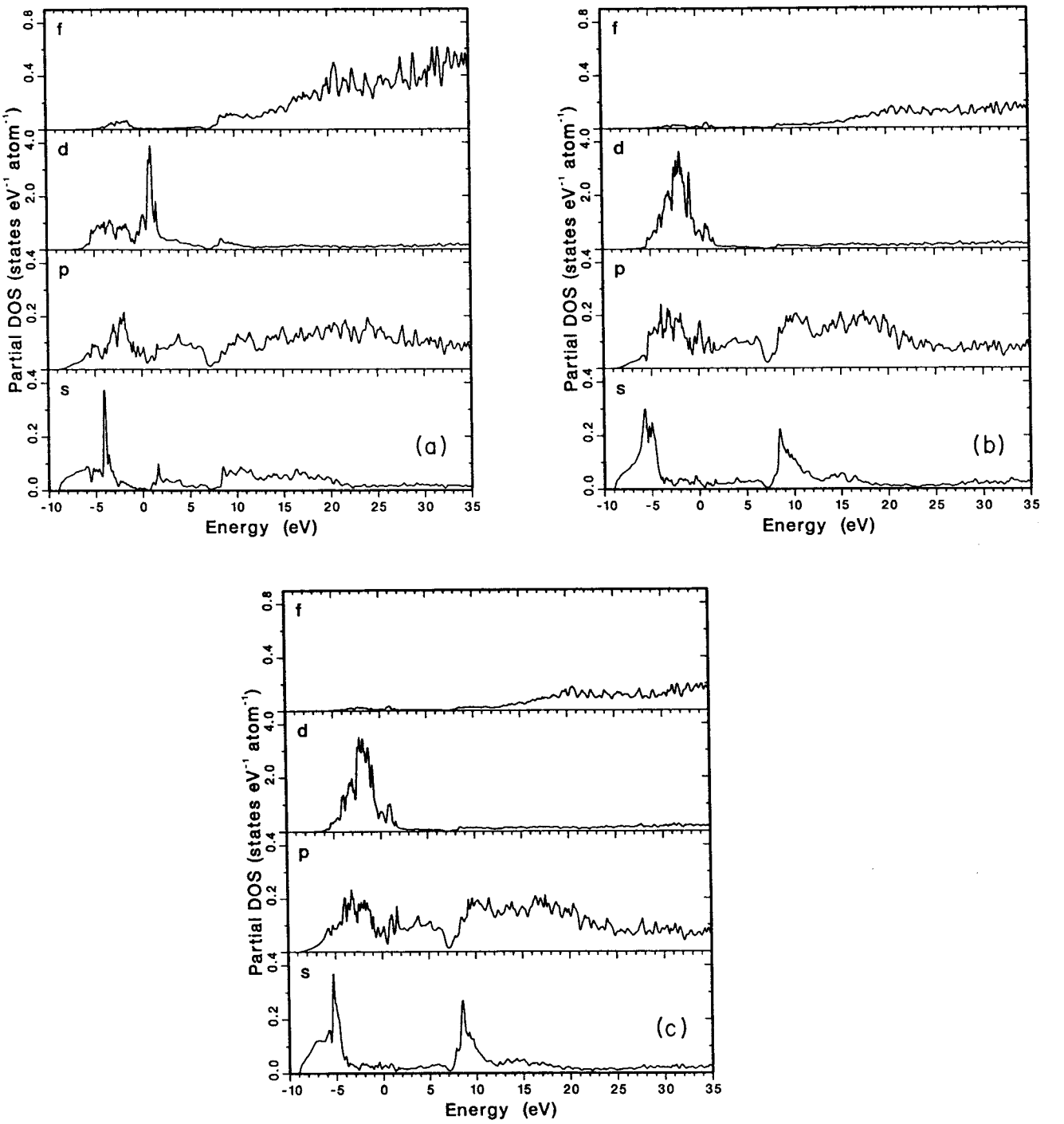

FIG. 1. Local partial density of states for $MoNi_3$ long-range-ordered orthorhombic alloy obtained with the extended basis set of LSW method: (a) Mo site; (b) Ni at Wyckoff position 2b; (c) Ni at Wyckoff position 4f. Fermi energy set to zero.

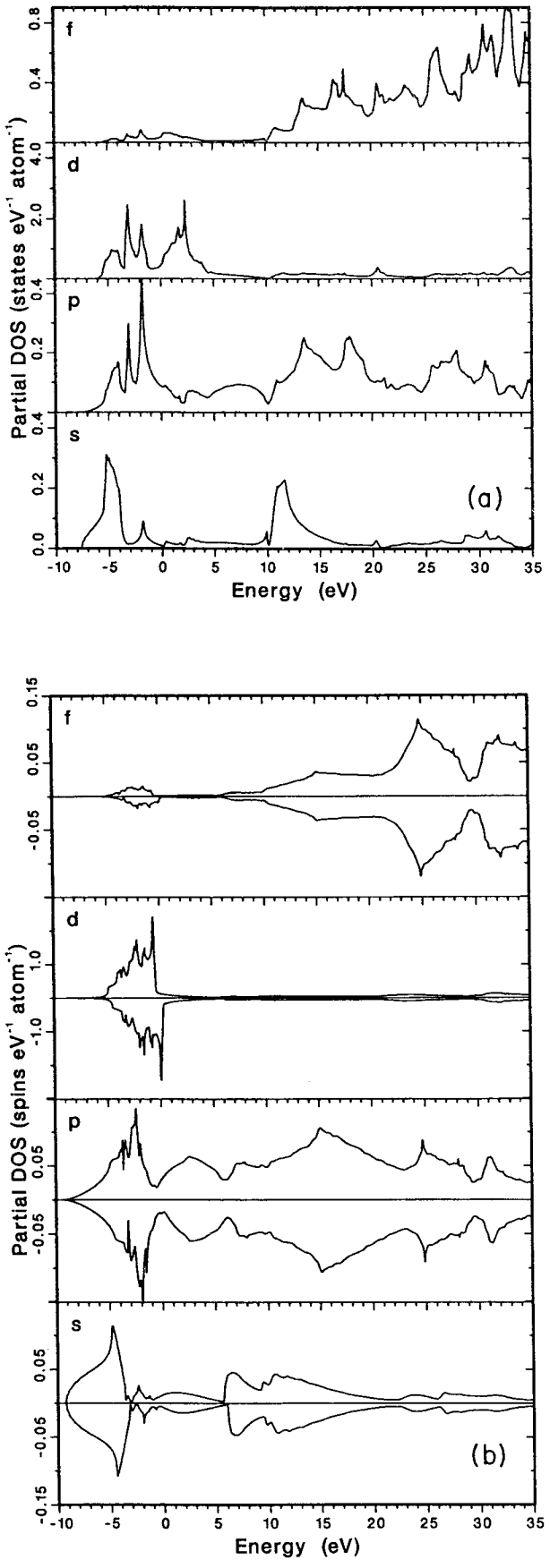

FIG. 2. Partial density of states of parent metals: (a) bcc Mo and (b) fcc ferromagnetic Ni. Fermi energy set to zero.

and isochromat bremsstrahlung spectra calculated on the basis of local partial states from Figs. 1 and 2 are given and are compared carefully with experimental findings.

IV. RESULTS AND DISCUSSION

A. X-ray absorption

Calculations of x-ray absorption at the K edge of Ni have been presented by several authors (e.g., see Ref. 18). In Fig. 3 our calculated and measured K edge of Ni in the range up to 70 eV from Fermi level are shown. Spectrum c was calculated in the single-particle model. It means that one $1s$ core electron was excited to an unfilled state of the initial, unperturbed crystal. The remaining electrons were assumed to be frozen in their original states. Therefore, the fine structure near the core-edge onset is expected to reflect directly the unoccupied DOS as symmetry projected by the dipole selection rule. In our case the K edge of Ni arises from the $1s$ to (unoccupied) p-like state transitions. The p-like DOS shown in Fig. 2(b) has been broadened by the convolution with the Lorentzian distribution to account for the $1s$ Ni core hole and final-state lifetime[19] and with the Gaussian distribution to account for the experimental resolution. The full width at half maximum parameters Γ_L and Γ_G were equal to $1.4+0.1(E-E_F)$ eV and 1.5 eV, respectively. The position of the Fermi energy on the experimental curve is not known; thus the experimental spectra have been aligned with theoretical curves to give the best overall match, here and consistently throughout the paper. The straggling tail of the theory curve should be ascribed to the energy dependence of the single-particle matrix element (which was neglected here), and to the lack of higher energy bands that contribute to the spectrum at lower energies through hot-electron broadening.[18] To account for this deficiency in the theory the continuous arctangent function was subtracted from the experimental curve (b in Fig. 3). This background correction brought the intensity of peaks in the observed and calculated spectra

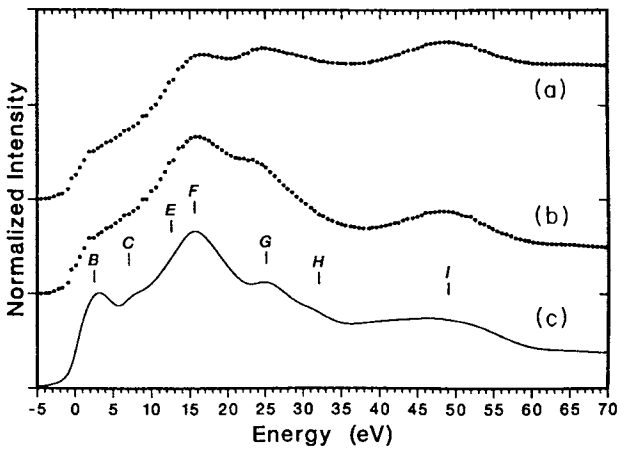

FIG. 3. X-ray absorption K edge of elemental Ni: (a), experimental spectrum; (b), experimental spectrum after background correction; (c), calculated spectrum.

to the same level. Apart from the fact that the intensity of peak B is overpronounced in the calculated spectrum, very good agreement between theory and experiment was obtained over the whole energy range.

The K edge of Ni in the orthorhombic $MoNi_3$ alloy is presented in Fig. 4, where a gives the direct experimental result while b shows the result after a background correction equivalent to that applied to pure Ni. The Ni atoms occupy two different positions in the orthorhombic unit cell. The p-like DOS for both positions are shown in Figs. 1(b) and 1(c). The K edges of Ni in both these positions calculated for the alloy in the same way as for pure Ni are shown in Fig. 4 as curves d and e. Curve c shows the K-edge spectrum properly weighting contributions from both types of atoms. The agreement between theory and experiment is not as good as for pure Ni. In particular, shoulder E is greatly overestimated and appears as a separated peak. In general, some differences can still be attributed to the core-hole potential and single-particle matrix elements which can differ in the alloy from those in pure metals. However, the high level of agreement between the experiment and K spectrum of pure Ni calculated on the basis of the ground-state partial DOS indicates that the influence of the core-hole potential on the unoccupied p-like states is small. Actually, this conclusion was rather expected because the main response to the hole (screening) should be made by the more localized $3d$ electrons which are the dominating part of the valence electrons. The same argument should hold in the case of the alloy.

One can gain a direct insight to the importance of the core-hole potential without referring to *ab initio* calculations by comparing the XAS and BIS spectra, since in the latter technique no core orbitals or holes are involved.

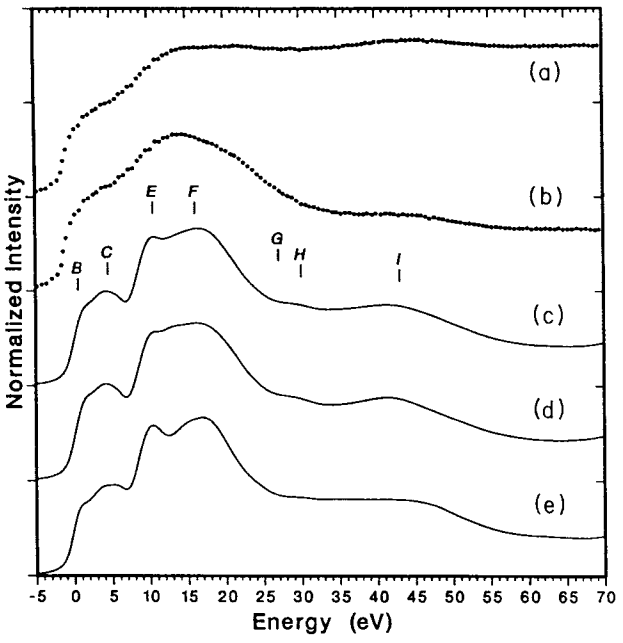

FIG. 4. K-absorption edge of Ni in the $MoNi_3$ alloy: (a), experimental spectrum; (b), experimental spectrum after background correction; (c), calculated spectrum of $MoNi_3$ orthorhombic alloy; (d), spectrum calculated for Ni at Wyckoff position 2b in the unit cell and (e), for Ni at Wyckoff position 4f.

B. Bremsstrahlung isochromat spectra

In the bremsstrahlung isochromat process the electron transition takes place between two states above the Fermi energy. There are no simple selection rules or site projection that can be used for the interpretation of spectra in terms of the local partial DOS. When we consider the incoming electron as a plane wave (with given kinetic energy) the shape of the BIS spectrum is determined by the superposition of all local partial DOS weighted by the appropriate transition matrix elements. It was shown in the case of the Ni isochromat spectra that these matrix elements change significantly when the energy of incoming electrons varies from 530 to 5415 eV.[6] Little systematic attention has been given, however, to the calculation of BIS transition matrix elements according to a physically realistic model in solids. Speier *et al.*[20] performed some calculations of the matrix elements depending on atomic number and angular momentum for incoming electron energy equal to the Al $K\alpha$ line (1487 eV) and for the energy region of the final electron states up to 26 eV. Simunek, Vacker, and Sobczak[21] studied the dependence of transition probability on angular quantum number for two energies of incoming electrons (1487 and 5415 eV) in the energy region 50–380 eV for Pd and Cu. Unfortunately, we did not succeed in reproducing the 5415-eV Ni and Mo isochromats in the energy range 0–40 eV using the above probabilities. Hahn and Rule[22] (HR) calculated the relative probabilities for electrons to be captured by an atomic or ionic system with different Z. Chu and Best[6] used their results to simulate the Ni isochromats for different energies of incoming electrons and found good agreement with the experimental results. We also used the transition probabilities obtained by the interpolation of data published by HR. The values that we used to weight the partial DOS of Ni and Mo in order to build the BIS spectra for kinetic energy of incoming electrons, 530, 1214, and 5415 eV, are reported in Table I. Curves resulting from this procedure were subse-

TABLE I. Relative probabilities of transition from continuum to given atomic function for different kinetic energies of the incoming electrons as obtained from Ref. 21. All entries were normalized by the probability value of transition to Ni $4s$ states for the energy 5415 eV.

	Atomic function	Kinetic energy of incoming electrons (in eV) 5415	1214	530
Mo	$5s$	1.25	4.39	7.61
	$5p$	0.99	8.26	18.72
	$4d$	0.34	8.51	29.33
	$4f$	0.02	1.63	9.14
Ni	$4s$	1	4.43	8.45
	$4p$	0.39	5.42	15.69
	$3d$	0.05	3.22	14.21
	$4f$	0	0.26	1.71

quently convoluted with the Lorentzian distribution with $\Gamma_L = 0.5 + 0.1(E - E_F)$ eV to account for the lifetime of the electron in the excited final state and with the Gaussian distribution with Γ_G=1.8 eV for the 5414-eV spectrum and Γ_G=0.5 eV for the 1214- and 530-eV spectra to simulate the experimental broadening (see Sec. II for experimental details). Spectra obtained this way are collected in Figs. 5(a) and 5(b). Dramatic changes of the relative contribution of *d*-like states are clearly visible in both cases when going from 530 to 5415 eV. In Figs. 6 and 7 we compare the theoretical BIS spectra for 5415 eV with our measurements for Ni and Mo, respectively. To account for the electrons which inelastically scatter prior to the radiative transition, we convoluted the energy loss spectra of Ni (Ref. 23) and Mo (Ref. 24) with the total DOS. The resulting curves do not show any pronounced structure. To compare the calculated and experimental BIS, one can add these contributions to the calculated BIS or subtract them from the experimental data. Curves *b* in Figs. 6 and 7 show the experimental spectra after subtracting the contribution from inelastically scattered electrons. The Ni isochromats have already been calculated[6,25] on the basis of the Ni DOS of Szmulowicz and Pease[18] but to the best of our knowledge, no such results were published for Mo in the wide energy

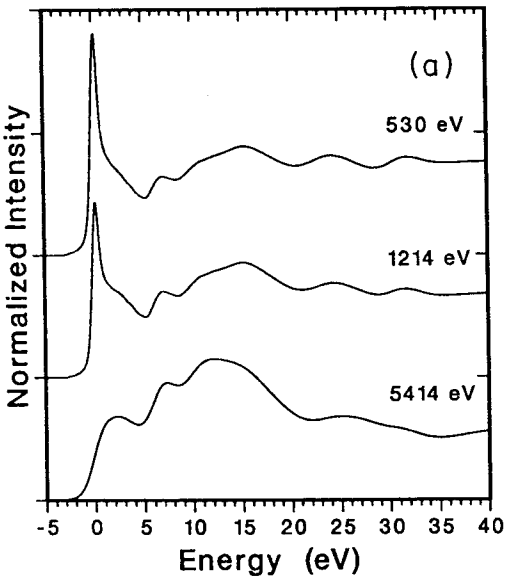

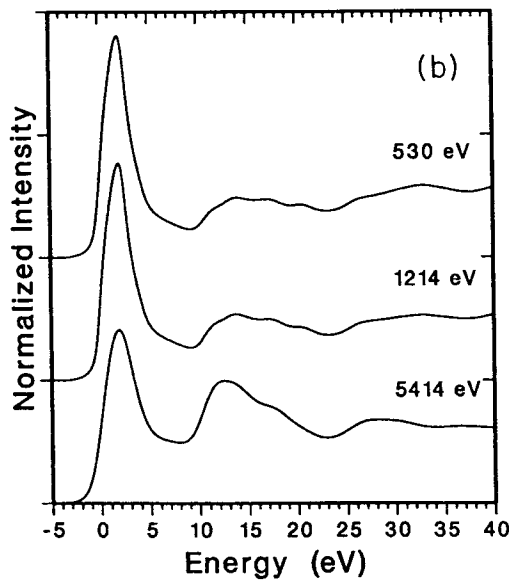

FIG. 5. Bremsstrahlung isochromat spectra of (a) Ni and (b) Mo for different kinetic energies of the incoming electrons as calculated from the partial DOS obtained in this work and the relative probabilities of transition based on Ref. 21.

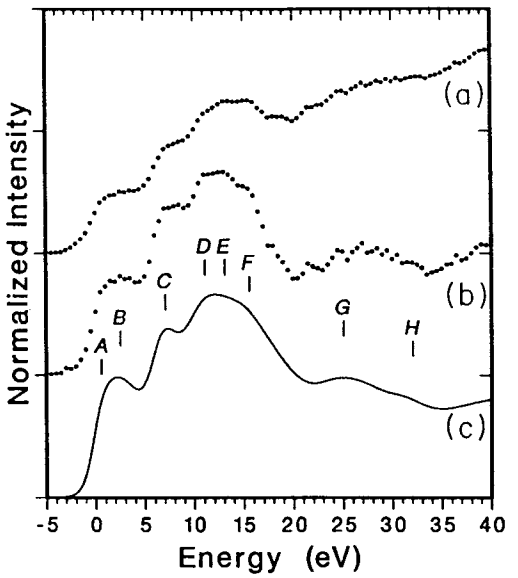

FIG. 6. The isochromat spectrum of Ni measured at the Cr $K\alpha$ line (5414.72 eV): (a), experimental spectrum; (b), experimental spectrum after subtraction of the inelastic electron contribution; (c), calculated spectrum (as in Fig. 5).

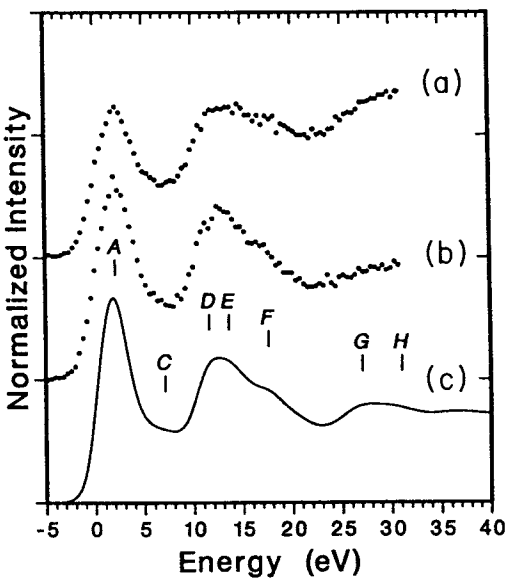

FIG. 7. The isochromat spectrum of Mo measured at the Cr $K\alpha$ line (5414.72 eV). All entries and explanations as in Fig. 6.

TABLE II. Main contribution to the structure of BIS spectra in terms of partial DOS. Features named as in Figs 6 and 7. Parentheses indicate relatively small contributions. All energies given in eV.

	Ni		Mo		$MoNi_3$	
Feature	Energy	States	Energy	States	Energy	States
A	0.5	*d*	2	*d*	1	*d* Mo (+*d* Ni)
B	2.5	*s* + *p*	0.5[a]	*p*	0.5[a]	*p* Mo (+*p* Ni)
C	7	*s* + *p*	7	*p*	4.5	*p* Mo + *p* Ni
D	11	*s*(+*p*)	11.5	*s*	9	*s* Ni (+*p* Ni +*s* Mo)
E	12.5	*s* + *p*	13.5	*p*	10.5	*p* Ni + *p* Mo
F	15.5	*p*	17.5	*p*	16[b]	*p* Ni + *p* Mo
G	25	*p*	27	*p*	27[c]	*p* Ni + *p* Mo
H	32	*p*	31	*p*	30[c]	*p* Ni + *p* Mo

[a]Overlaid by feature *A*, not visible.
[b]Misplaced by about 3 eV.
[c]Poorly reproduced.

range of the final states and, in particular, for the 5415-eV transition energy. We would like to stress the excellent overall agreement in both cases between calculated and measured spectra as well as the perfect matching of all structures indicated in Figs. 6 and 7. This proves the reliability of our *ab initio* calculation of partial DOS in the wide range of energy. It also shows that the transition probabilities obtained from the atomic model of HR are satisfactorily accurate for solids.[26] Close inspection of the spectra presented in Figs. 6 and 7 shows that all the indicated features can be traced back to the respective partial DOS in Figs. 2(a) and 2(b). A summary of such assignments is given in Table II. Before we move to the discussion of the isochromat spectrum of orthorhombic $MoNi_3$ alloy we would like to draw the reader's attention to Fig. 3 and to compare it with Fig. 6 and Table II. All features found in BIS spectrum which contain sufficient contribution from *p*-like states can also be found at the *same* energy position in the x-ray *K*-edge absorption spectrum. This agreement gives an experimental upper bound for possible core-hole effects in the *K*-edge Ni spectrum.[27]

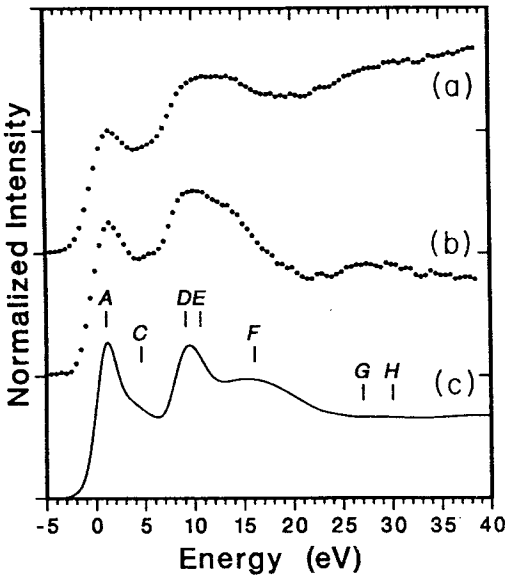

FIG. 8. The isochromat spectrum of orthorhombic $MoNi_3$ alloy measured at the Cr $K\alpha$ line (5414.72 eV). All entries and explanations as in Fig. 6.

In Fig. 8, organized similarly as Figs. 6 and 7, we present BIS spectrum of the orthorhombic $MoNi_3$ alloy together with theoretical curves obtained in the same way as for the parent metals. We used the same relative transition probabilities (listed in Table I) for weighting the local partial DOS of $MoNi_3$ [Figs. 1(a), 1(b), and 1(c)]. Contrary to the good agreement between theory and experiment obtained for pure Ni and Mo, there is an obvious discrepancy in the energy range from 8 to 20 eV in the spectra of the alloy. To exclude the possibility that the discrepancy is caused by uncertainties in the transition probabilities, we performed a simulation treating these probabilities as adjustable coefficients. Only an insignificant improvement could be obtained this way. Furthermore, the discrepancies in Fig. 8 correlate well in the energy range with the disagreement seen in Fig. 4. The only conclusion from this consideration, and from the discussion above where we ruled out significant influence of the core hole on Ni *K* x-ray absorption spectrum, is that the partial DOS of $MoNi_3$ alloy is not correct. In our opinion this is not due to the failure of *ab initio* calculations.[28] On the contrary, from these calculations we conclude that although $MoNi_3$ alloy possesses a high degree of long-range orthorhombic order (as reported in Sec. II), the local structure must deviate substantially from this symmetry, causing the discrepancy. We can distinguish two reasons for this deviation. The first is the presence of substitutional (or chemical) disorder. We can form different crystal structures by various heat treatments of the alloy with the same concentration of elements. Even the amorphous structure for $MoNi_3$ alloy can be easily formed by radio frequency co-sputtering. The random (substitutionally disordered) $MoNi_3$ alloy crystallizes in the fcc lattice. Study of the occupied band structure on the basis of calculations and x-ray emission spectra showed a tendency to form local structures similar to $L1_2$ type (as in $AuCu_3$) in such random $MoNi_3$ alloy.[29] After annealing of

the random fcc alloy during several days at temperatures below 1100 K, the intermetallic compound with the superlattice with orthorhombic symmetry is formed.[15] This means that every Ni and Mo atom can be found in its own sublattice. However, this long-range order can be perfect only at zero temperature. Thus the same disorder in the positions of Ni and Mo atoms is always expected. The second reason, being a consequence of the first one, is a local deformation of the sublatticies which is caused by the size effect (the difference in size of Mo and Ni atoms), when a given atom does not occupy its own sublattice. A similar situation was already found in the III-V and II-IV semiconducting pseudobinary (ternary) alloys.[30,31] A perfect zinc-blende symmetry was always seen by the x-ray diffraction experiments for these random alloys. But essential discrepancies were noticed between the near-neighbor distances resulting from x-ray diffraction and extended x-ray absorption fine-structure (EXAFS) measurements[30] which were explained successfully by a model of local deformation of the lattice.[31] Very recently this problem was again extensively discussed by Su-Huai Wei and Zunger[32] in the case of II-VI semiconducting alloys. They have shown that changes in the electronic structure of the alloy induced by both effects named above (substitutional disorder and local lattice deformation) are distinguishable and of equal importance. In order to resolve the problem of local structure in the ordered $MoNi_3$ alloy, the EXAFS measurements of the ordered and disordered $MoNi_3$ alloys have been already performed. A quantitative analysis of the EXAFS data is in progress and will be published elsewhere.

V. SUMMARY

We have reported the systematic study of the unoccupied states of ordered $MoNi_3$ alloy using its parent metals as reference. The investigation included (i) BIS measurements for photon energy equal to 5415 eV in the wide energy range; (ii) Ni K-edge x-ray absorption measurements; (iii) *ab initio* electron band-structure calculations for the alloy and metals over a wide energy range above the Fermi energy; (iv) calculation of all measured spectra.

Next, the careful comparison of theoretical and experimental results for metals has shown excellent agreement in the wide range of energy. This enabled us to make the following conclusions: (i) the LSW method with the extended basis set proves to be suitable and accurate for calculation of the electronic structure in the wide range of energy above the Fermi energy (without losing its intrinsic efficiency); (ii) bremsstrahlung transition probabilities obtained from HR atomic (ionic) model are satisfactorily accurate also in solids; (iii) core-hole effects in the Ni K-edge x-ray absorption spectrum are negligibly small.

Finally, on the basis of the systematic discrepancy between experimental results and *ab initio* calculations performed under the assumption of long-range orthorhombic ordering in $MoNi_3$ alloy, we have suggested that the real local structure of this alloy differs considerably from the orthorhombic structure. The x-ray diffraction shows the spatial average of the atomic order but the electronic structure is sensitive to local atomic environment. An analogy to the III-V and II-VI pseudobinary (ternary) semiconducting alloys has been drawn.

ACKNOWLEDGMENTS

This work was financially supported in part by the Nederlandse Organisatie voor Wetenschappelijk Onderzoek and in part by the CPBP 01.04 program.

[1] J.K. Lang and Y. Baer, Rev. Sci. Instrum. **50**, 221 (1979).
[2] J.K. Lang, Y. Baer, and P.A. Cox, J. Phys. F **11**, 121 (1981).
[3] M.T. Czyżyk and R.A. de Groot, in *2nd European Conference on Progress in X-Ray Synchrotron Radiation Research*, edited by A. Balerna, E. Bernieri, and S. Mobilio (Italian Physical Society, Rome, 1990), Vol. 25, p. 47.
[4] P.J.W. Weijs, M.T. Czyżyk, J.F. van Acker, W. Speier, J.B. Goedkoop, H. van Leuken, H.J.M. Hendrix, R.A. de Groot, G. van der Laan, K.H.J. Buschow, G. Wiech, and J.C. Fuggle, Phys. Rev. B **41**, 11 899 (1990).
[5] B.R.A. Nijboer, Physica **12**, 461 (1946).
[6] C.C. Chu and P.E. Best, Phys. Rev. B **19**, 3414 (1979).
[7] W. Speier, R. Zeller, and J.C. Fuggle, Phys. Rev. B **32**, 3597 (1985).
[8] H.J.W.M. Hoekstra, W. Speier, R. Zeller, and J.C. Fuggle, Phys. Rev. B **34**, 5177 (1986).
[9] E. Sobczak and J. Auleytner, Phys. Rev. B **37**, 6251 (1988).
[10] By the minimal basis set in the LMTO and ASW-LSW methods we understand the set which includes one radial augmenting function for each value of the orbital quantum number.
[11] The localized spherical-wave method of electronic structure calculation is a version of the well-known augmented-spherical-wave method and has been already used in different cases, see, e.g., Refs. 12, 13, 3, and 4. The formalism of method has been recently described by H. van Leuken, A. Lodder, M.T. Czyżyk, F. Springelkamp, and R.A. de Groot, Phys. Rev. B **41**, 5613 (1990).
[12] M.T. Czyżyk, R.A. de Groot, G. Dalba, P. Fornasini, A. Kisiel, F. Rocca, and E. Burattini, Phys. Rev. B **39**, 9831 (1990).
[13] J. Ghijsen, L.H. Tjeng, J. van Elp, H. Eskes, J. Westerink, G.A. Sawatzky, and M.T. Czyżyk, Phys. Rev. B **38**, 11 322 (1988); M. Grioni, M.T. Czyżyk, R.A. de Groot, J.C. Fuggle, and B.E. Watts, *ibid.* **39**, 4886 (1989).
[14] S. Satio and P.B. Beck, Trans. Metal. Soc. AIME **215**, 938 (1959).
[15] R.E.W. Casselton and W. Hume-Rothery, J. Less-Common Met. **7**, 212 (1964).
[16] V.L. Moruzzi, J.F. Janak, and A.R. Williams, *Calculated Electronic Properties of Metals* (Pergamon, New York, 1978).
[17] K. Ławniczak-Jabłońska and M.T. Czyżyk (unpublished).

[18] F. Szmulowicz and D.M. Pease, Phys. Rev. B **17**, 3341 (1978).
[19] J.E. Muller, O. Jepsen, and J.W. Wilkins, Solid State Commun. **42**, 365 (1982).
[20] W. Speier, J.C. Fuggle, P. Durham, R. Zeller, R.J. Blake, and P. Sterne, J. Phys. C **21**, 2621 (1988).
[21] A. Simunek, J. Vacker, and E. Sobczak, Phys. Rev. B **38**, 8515 (1988).
[22] Y. Hahn and D. Rule, J. Phys. B **10**, 2689 (1977).
[23] J.L. Robins and J.B. Swan, Proc. Phys. Soc. London **76**, 857 (1960).
[24] G. Gergely and M. Menyhard, J. Electron Spectrosc. Relat. Phenom. **28**, 279 (1989).
[25] K. Ławniczak-Jabłońska, in *Inner-Shell and X-Ray Physics of Atoms and Solids*, edited by D.J. Fabian, H. Kleinpoppen, and L.M. Watson (Plenum, New York, 1981), p. 523.
[26] To further examine the accuracy of HR's atomic or ionic model in the estimation of the probability of BIS transitions in solids, we have used HR results to obtain transition probabilities for Ti and Si for energy 1487 eV. Then, a theoretical BIS spectrum of the compound TiSi was calculated with local partial DOS taken from P.J.W. Weijs, M.T. Czyżyk, J.C. Fuggle, W. Speier, D.D. Sarma, and K.H.J. Buschow, Z. Phys. B **78**, 423 (1990). We obtained good agreement with experiment within the entire range energy in the experimental data available to us (that was up to 15 eV above Fermi energy).
[27] There might be, however, non-negligible effects of the core-hole potential on magnetic x-ray dichroism of K edge in Ni metal.
[28] We mean here that there is no reason for any strong many-body effects that could possibly disable the one-particle description of BIS process. Even in the case of strongly correlated valence electrons, as in CuO, BIS spectra can be properly described by the one-particle process, as one may see in Ref. 13.
[29] K. Ławniczak-Jabłońska, S. Mobilio, J. Inoue, and K. Tohyama, in *2nd European Conference on Progress in X-Ray Synchrotron Radiation Research* (Ref. 3), p. 701.
[30] J.C. Mikkelson and J.B. Boyce, Phys. Rev. Lett. **49**, 1412 (1982); Phys. Rev. B **28**, 7130 (1983).
[31] A. Balzarotti, N. Motta, A. Kisiel, M. Zimnal-Starnawska, M.T. Czyżyk, and M. Podgórny, Phys. Rev. B **31**, 7526 (1985).
[32] Su-Huai Wei and A. Zunger, Phys. Rev. B **43**, 1662 (1991).